International Journal of Nanomedicine

Dovepress
open access to scientific and medical research

Open Access Full Text Article

ORIGINAL RESEARCH

Ultrasound-Assisted Preparation of Exopolysaccharide/Nystatin Nanoemulsion for Treatment of Vulvovaginal Candidiasis

This article was published in the following Dove Press journal:
International Journal of Nanomedicine

Ruiteng Song[1]
Fang Yan[1]
Min Cheng[2]
Fakun Dong[1]
Yongqi Lin[1]
Yuzhen Wang[3]
Bo Song[1]

[1]School of Pharmacy, Weifang Medical University, Weifang, Shandong 261053, People's Republic of China; [2]Clinical Medical College, Weifang Medical University, Weifang, Shandong 261053, People's Republic of China; [3]Medical Imaging Specialty, Weifang Medical University, Weifang, Shandong 261053, People's Republic of China

Purpose: As one of the classic anti-*Canidia albicans* (CA) and vulvovaginal candidiasis (VVC) drugs, nystatin (NYS) is limited by poor water solubility and easy aggregation. Traditional NYS vaginal delivery formulations do not fully adapt to the specific environment of the vaginal cavity. The use of exopolysaccharides (EPS) has great application potential in emulsifiers, but its use has not been reported in nanoemulsions. In this work, an EPS/NYS nanoemulsion (ENNE) was developed to improve the activities of NYS against CA and VVC

Methods: The ENNE was prepared by ultrasonic method using EPS as an emulsifier, liquid paraffin oil as an oil phase, PEG400 as a co-emulsifier, and NYS as the loaded drug. ENNE preparation was optimized by response surface method. After optimization, in vitro and in vivo analysis of the anti-CA activity; animal experiments; staining with propidium iodide (PI), periodic acid-schiff (PAS), and hematoxylin-eosin (H&E); and cytokine experiments were performed to investigate the therapeutic ability against VVC.

Results: The optimal formulation and preparation parameters of ENNE were determined as follows: EPS content of 1.5%, PEG400 content of 3.2%, NYS content of 700 μg/mL, paraffin oil content of 5.0%, ultrasonic time of 15 min, and ultrasonic amplitude of 35%. The ENNE showed an encapsulated structure with an average particle size of 131.1 ± 4.32 nm. ENNE exhibited high storage and pH stability, as well as slow release. The minimum inhibitory concentration (MIC) of ENNE against CA was only 0.125 μg/mL and the inhibition zone was 19.0 ± 0.5 mm, for greatly improved anti-CA effect. The prepared ENNE destroyed the membrane of CA cells, and exhibited good anti-CA effect in vivo and therapeutic ability against VVC.

Conclusion: The results of this study will promote the application of EPS in nanotechnology, which should lead to new and effective local drug formulations for treating VVC.

Keywords: *Canidia albicans*, ultrasonic, response surface method, antifungal

Introduction

Vulvovaginal candidiasis (VVC) is a serious gynecological disease that is mainly caused by *Canidia albicans* (CA) infection.[1] Currently, most treatment of VVC is based on nystatin (NYS), fluconazole, and amphotericin B.[2]

NYS is commonly used for the prevention and treatment of VVC and is the first antifungal conjugated polyene macrolide drug.[3] However, NYS has significant two disadvantages: (1) NYS administrated orally is not absorbed in the gastrointestinal tract, and can result in adverse gastrointestinal reactions, such as fever, diarrhea, nausea and upper abdominal pain;[4] (2) NYS is insoluble in water and can easily accumulate,

Correspondence: Yuzhen Wang; Bo Song
Weifang Medical University, Baotong Street, No. 7166, Weifang, Shandong 261053, People's Republic of China
Tel +86-536-8462490
Email wangyz@wfmc.edu.cn; songsbob@163.com

submit your manuscript | www.dovepress.com
DovePress
http://doi.org/10.2147/IJN.S241134

seriously affecting its stability, pharmacodynamics, and bioavailability.[5] As an alternative, NYS is made into suppositories, gels, creams and emulsions for local drug delivery. However, these conventional dosage forms often have insufficient adhesion and permeability, leading to limited function in the special environment and structure of the vagina.[6] Additionally, incomplete treatment may allow residual fungi in the mucosal fold of the vagina, leading to disease recurrence.

Nanoemulsions offer advantages of improving drug dispersion, promoting drug absorption, extending action time, reducing dose and reducing toxicity, and are suitable for treatment of local inflammation and infection.[7,8] Nanoemulsions are transparent or semi-transparent liquids composed of water, oil, emulsifiers, and co-emulsifiers, and are dozens to hundreds of nanometers in size. Nanoemulsions are thermodynamic-stabilizing systems, and have a low surface tension. Nano-scale droplets will produce a larger specific surface area and enhance drug dispersion and efficacy.[9] Commonly used emulsifiers include Span 80, Tween 80, and phospholipids, but ordinary emulsions require higher amounts of emulsifiers than nanoemulsions, possibly causing toxicity. Therefore, safer emulsions prepared with lower amounts of safer emulsifying agents are required.

Bacterial exopolysaccharides (EPS) are high molecular weight polymers with adhesion properties that are naturally secreted by bacteria. Remarkable properties of emulsification, water retention, gelation, biodegradability and biocompatibility have led to the wide use of EPS in food, medicine, and other fields.[10] EPS have outstanding emulsifying activity, indicating good application prospect for use of EPS as an emulsifier. Recently, EPS have been applied in nanotechnology. For example, EPS produced by *Lactobacillus plantarum* LCC-605 strain isolated from kimchi were used to prepare degradable nanoparticles for biological antifouling, such as the adsorption of heavy metal ions.[11] However, there has been no report on the application of EPS in nanoemulsions.

Ultrasonic emulsification can break larger oil droplets through cavitation, the implosion of bubbles, and microjet formation, allowing emulsifiers to be adsorbed on smaller oil droplets and form nanoemulsions.[12] Ultrasonic emulsification can also be used to adjust the dispersion degree of droplets by controlling ultrasonic frequency and time, using a treatment procedure that is rapid and simple to operate.[13]

EPS/NYS nanoemulsion (ENNE) was prepared using ultrasound-treated EPS from *Bacillus vallismortis* WF4 as an emulsifier. The response surface method was used to optimize the preparation of nanoemulsions on the basis of droplet size, zeta potential, inhibition zone, and drug release in vitro. The physico-chemical properties and the in vivo and in vitro anti-CA activities of ENNE were further studied. Additionally, the anti-CA and therapeutic effects of ENNE on VVC were investigated in animal experiments. The results of this study provide the basis for further application of EPS in nanoemulsion technology and demonstrate a reasonable strategy to improve the shortcomings of NYS and enhance treatment of VVC.

Materials and Methods

Materials, Reagents and Animals

EPS (molecular weight of 3.83×10^5 Da; composition of monosaccharides was mannose/glucose/xylose/arabinose = 51.77%/20.82%/13.28%/14.13%) was derived from fermentation products of the *B. vallismortis* WF4 strain.[14] A single batch of EPS was used for all experiments presented here. Peptone 10.0 g/L, yeast extract 10.0 g/L, and glucose 5.0 g/L (pH = 6.5–7.0) were combined and used as fermentation medium. Sunflower oil, soybean oil, peanut oil, and corn oil were purchased from Shandong Luhua Group Co., Ltd., China (date of manufacturing was within six months of the date of the experiment). NYS, ethanol, isopropanol, n-butanol, PEG200, PEG400, Tween 80, and liquid paraffin oil were purchased from Shanghai Macklin® Reagent Co., LTD., China. *C. albicans* (2E00856) was obtained from the Bena Culture Collection (BNCC) and cultured in Martin medium (peptone 5.0 g/L, yeast extract 2.0 g/L, glucose 20.0 g/L, magnesium sulfate 0.5 g/L, dipotassium phosphate 1.0 g/L, pH = 6.2–6.6) at 37°C and 180 rpm. Estradiol Benzoate Injection was obtained from Shanghai Quanyu Biotechnology Animal Pharmaceutical Co. LTD. China. Propidium iodide (PI), Periodic acid-Schiff (PAS), Hematoxylin and Eosin (H&E) kits were obtained from Solarbio. ELISA kits for TNF-α, IL-6, IL-1β, and IL-10 were purchased from Sigma. Positive control drug (nifuratel-NYS vaginal cream) was provided by Nanjing Nanda Pharmaceutical Co. LTD. China). The mice were obtained from the Laboratory Animal Center of Weifang Medical University.

Preparation of ENNE

NYS Solubility

The solubility of NYS in co-emulsifiers (ethanol, isopropanol, n-butanol, PEG200, PEG400, and Tween 80), oil phase (soybean oil, peanut oil, sunflower seed oil, corn oil and liquid

paraffin oil) and distilled water was determined according to the methods of Sosa et al.[13] Briefly, excess NYS was dissolved in different solvents, and stirred at 37°C in water bath for 72 h avoiding light. The solution was then centrifuged at 12,000 rpm for 1 h, diluted with methanol, and ultrasonicated for 20 min. Absorbance at 314 nm was measured after filtration with 0.22 μm microporous membrane. The solubility was calculated according to the standard curve ($y = 10.697x + 0.7493$, $R^2 = 0.9992$). Each experiment was repeated in triplicate.

Preparation of Nanoemulsions by Ultrasound

Nanoemulsions were prepared by ultrasound treatment with EPS as an emulsifier, PEG400 as a co-emulsifier, liquid paraffin oil as an oil phase, and NYS as the drug. EPS was dissolved in distilled water, then PEG400 was added and vortexed (QL-901, China, Aomen) for 5 min. NYS was weighed and dissolved in liquid paraffin oil, and added into the EPS solution and vortexed for 5 min to obtain raw EPS/NYS emulsions. The emulsions were ultrasonicated (SONICS, VCX750) using a 3 mm diameter probe and an interval time of 5 s on, 5 s off. Throughout the ultrasound treatment, the container containing the sample was in an ice bath, and temperature difference in the system was less than 20°C.

Optimization of Nanoemulsion Preparation by Response Surface Method

Ultrasonic treatment conditions and the emulsion formulation were optimized by full factorial design of response surface method, including six factors: NYS content, ultrasonic treatment time, ultrasonic treatment amplitude, emulsifier amount, co-emulsifier amount, and oil phase volume. For each factor, three levels were selected (Table 1A): low (−1), medium (0) and high (1). First, the influences of NYS content, ultrasonic time, and ultrasonic amplitude on droplet size were studied in liquid paraffin oil. The amounts of EPS, PEG400, and liquid paraffin oil were set as 0.5% (w/w), 2.0% (w/w), and 15.0% (w/w), respectively. Twenty-seven samples were processed in triplicate according to a full factorial design (3 ×3 ×3). Particle size was measured, and mean value and standard deviation (SD) were calculated. After determining the optimal ultrasonic treatment time, the optimal ultrasonic amplitude and NYS content in the liquid paraffin oil were determined. The effects of EPS, PEG400, and liquid paraffin oil content on the particle size of the nanoemulsion, zeta potential, inhibition zone, and in vitro release of NYS were investigated. Thirty-two samples were processed according to a new full factorial design (3 ×3 ×3 + 5). Response value was measured, and mean values and SD were calculated for triplicate samples. Finally, Design expert® (version 11.1.0.1, Stat-Ease, Minneapolis, USA) was used to conduct nonlinear regression analysis on the response, establish a mathematical model, and draw a 3-D response diagram.[12] The optimal process parameters and formulation were determined according to the target values of variables presented in Table 1B.

Table 1 (**A**) Selected Independent Variables and Their Levels; (**B**) Constraints Applied on Variables

Independent Variables	Levels		
	Low (−1)	Medium (0)	High (1)
X_1=NYS (μg/mL)	300	500	700
X_2=Time (min)	5	10	15
X_3=Amplitude (%)	15	25	35
X_4=EPS (%)	0.5	1	1.5
X_5=PEG400 (%)	0	2	4
X_6=Liquid paraffin oil (%)	5	15	25
Independent variables	Goals		Importance
X_1=NYS (μg/mL)	Maximize		+ + + + +
X_2=Time (min)	In range		– – – – – – – – – –
X_3=Amplitude (%)	In range		– – – – – – – – – –
X_4=EPS (%)	In range		– – – – – – – – – –
X_5=PEG400 (%)	In range		– – – – – – – – – –
X_6=Liquid paraffin oil (%)	In range		– – – – – – – – – –
Dependent variables			
Y_1=Droplet size (nm)	Minimize		+ + + + +
Y_2=ζ -potential (mV)	Maximize		+ + + + +
Y_3=Inhibition zone (mm)	Minimize		+ + + + +
Y_4=NYS released in 1h (%)	Maximize		+ + + + +

Physico-Chemical Characterisation of ENNE

Determination of Nanoemulsion Type

The type of nanoemulsion was determined by staining with methylene blue (2.0 mg/mL in ethanol) and Sudan red III (1.0 mg/mL in ethanol), which exhibit different diffusion velocities in nanoemulsions.[16] The two dyes (100.0 μL

each) were added into 3.0 mL of ENNE and diffusion was observed after 1 h.

Droplet Size, Zeta Potential, and Micromorphology

Particle size distribution and zeta potential were measured using a Zetasizer Nano ZS90 instrument (Malvern Instruments LTD., Malvern, U.K). Before measurement, the sample was diluted with distilled water (1:100 v/v) to avoid multiple scattering effect.[17,18] The micromorphology was then observed using a transmission electron microscope (TEM, HITACHI, HT7700, Japan).[19] Briefly, copper mesh containing ENNE was negatively stained with 2.0% phosphotungstic acid for 30 min, dried, and observed.

Encapsulation Efficiency (EE)

ENNE (3.0 mL) were centrifuged at 18,000 rpm (4°C, 10 min) with a high speed freezing centrifuge (3–30k, Sigma, Germany). The supernatant was diluted with methanol, and measured at the wavelength of 314 nm by UV spectrophotometer (UV-800a, Shanghai Yuanxi Instrument Co., LTD. China). The NYS content was calculated by substituting into the standard curve. The EE was calculated from Equation (1):[20]

$$EE(\%) = \frac{\text{Weight of loaded NYS}}{\text{Weight of initial NYS}} \times 100 \qquad (1)$$

Viscosity

The dynamic viscosity of ENNE was measured using a Brookfield DV–III viscometer (LV3 rotor). Briefly, 20 mL of ENNE was added into the sample cup at a speed of 20 rpm and torque of 20–80%. Each sample was measured three times and the average value was calculated (measured at a temperature of 25°C).

Differential Scanning Calorimetry (DSC) and Thermogravimetric Analysis (TG)

DSC was used to determine whether the drug was completely dissolved in the nanoemulsion.[15] Briefly, 2.0 mg sample was placed in a pan and the other pan was kept empty and used for reference. The temperature range of the instrument was set as 30 –200°C, the rate of increase in temperature was recorded as 10°C/min., and the flow of nitrogen in was maintained at 60 mL/min.

Stability

Samples of 3.0 mL ENNE were stored at 25°C in the dark for 10 weeks, and particle size was measured every two weeks to investigate the storage stability of ENNE. In separate experiments, 30.0 μL of ENNE was added to 3.0 mL distilled water adjusted to different pH (2, 3, 4, 5, 6, and 7). The change in particle size was measured after 6 h to assess the sensitivity of ENNE to pH.

Drug Release in vitro

The method to monitor in vitro release was modified from one described by Kassem et al.[21] Briefly, a dialysis bag containing 5.0 mL ENNE (3500 Da) was placed in 100 mL methanolic citrated-distilled water (30/70%) at pH = 4.5 (37°C water bath). A sample of 2.0 mL release medium was collected, and equivalent release medium was supplemented at 1, 2, 4, 8, 12, 24, 36, 48 and 60 h, respectively. The absorbance at 314 nm was determined after filtration through a 0.22 μm membrane. The content of NYS was calculated, and Origin 9.0 pro was used to construct an in vitro release profile. Experimental data were fitted to three kinetic models (zero order, first order, and Higuchi) by nonlinear least-squares regression using specialized software (Origin® version 9.0 pro., OriginLab, Northampton, Massachusetts, USA). The appropriateness of model fitting was determined by calculation of the correlation coefficient (r).

Anti-CA Assay in vitro

Minimal Inhibitory Concentration (MIC)

The MIC of ENNE to CA was determined using a double dilution method.[14] CA colonies were cultured in Martin liquid medium at 37°C at 180 rpm for 12 h, and centrifuged at 5000 × g for 5 min. The yeast were collected and washed three times with saline. Four groups were set: free NYS (NYS/oil, NYS/water), ENNE group, and blank emulsion group. Ten tubes with liquid medium were prepared for each group, and samples were added into each tube for final drug concentrations of 64, 32, 16, 8, 4, 2, 1, 0.5, 0.25, and 0.125 μL/mL. The prepared CA samples were added to concentrations of 1.0×10^5 CFU/mL, incubated in a shaker at 37°C for 18 h, and then the transparency of each tube of culture solution was observed visually. The absorbance at 600 nm was measured using a microplate reader (BIOTEK POWERWAVE XS US). The experiment was performed in triplicate.

Inhibition Zone

An inhibition zone experiment was conducted using the Oxford cup method.[22] Sterile saline was used to dilute the CA suspension to $OD_{630nm} = 0.05$. A small amount of the fungal suspension was evenly smeared on Martin solid

medium plate with sterilized cotton swabs, placed with Oxford cups, and then NYS/oil, NYS/water, ENNE, amphotericin B/water (positive control,) and blank nanoemulsions were added (drug concentrations in the drug groups were 50.0 μL/mL), respectively. The inhibition zone was observed and measured after 24 h-culture at 37°C.

Effect of ENNE on CA by Scanning Electron Microscope (SEM)

The CA in the clear zone boundary (described above) were stained and fixed with glutaraldehyde at 3.0% for 24 h. The effects of ENNE on CA cells were observed by scanning electron microscope (JSM-840, JEOL, Japan).

VVC Animal Experiments

Establishment of VVC Model in Mouse

All animal treatments and laboratory procedures were conducted according to the National Institutes of Health Guide for the Care and Use of Laboratory Animals (NIH Publications No. 8023, revised 1978), and approved by the Ethics Committee of Weifang Medical University (2019SDL049). A high estrogen level can affect the natural antifungal ability of the vaginal mucosa, leading to thickening and keratinization of the vaginal epidermis. This promotes the adhesion of CA and transformation into mycelium phase to penetrate into the cuticle, allowing proliferation in large quantities, which results in toxicity and inflammation. Therefore, regular estrogen supplementation during the construction of VVC mouse model can promote success of modeling.[23] A sufficient amount of clean grade ICR (Institute of Cancer Research) female mice (weight 20.0 ± 1.0 g) were subcutaneously injected with 1.2 mg/kg estradiol valerate after one week every two days before CA inoculation to induce false estrus conditions until the end of the experiment. After one week, 20.0 μL CA glycerin suspension was inoculated (the CA strain was cultured in liquid Martin medium and grown to logarithmic phase, and then centrifuged at 1000 rpm for 10 min. The yeast were washed twice with distilled water, and then suspended in 30% glycerol to a final concentration of 10^7 CFU/mL). The cell count was determined using a dilution plating method. After 5–7 days of inoculation, if redness and swelling in the vulva and white and thick secretions were observed, smear microscopy was performed. If the CA cells exhibited pseudohyphae and visible germ tubes, the modeling was successful.

In vivo Dynamic Resistance to CA

The successfully modeled mice were randomly assigned into four groups (n = 15): model group, ENNE group, positive control group (nifuratel-NYS vaginal cream), and blank group (normal saline). Each mouse received treatments by vaginal perfusion (50.0 μL) on days 1, 6, and 16. During treatment administration, sterile cotton swabs were applied to collect the vaginal secretions of mice every three days. The head of the cotton swab was cut off, placed in 1.0 mL sterilized normal saline, and then diluted ten-fold. Then, 50.0 μL the solution was evenly smeared on Martin solid medium. After incubation at 37°C for 1 day, the number of fungi were counted (CFU mL^{-1}). The CA colony count generated on the solid medium represents the count of living fungi in the vagina of mice, which can be used to assess the fungi load quantity in the body. A steady count of 10^3 CFU/mL is considered the uninfected and nonsymptomatic CA count.[24]

PI Staining

The lethal effect of ENNE on CA in vivo was studied by PI fluorescence staining.[14] The vaginal secretions of mice in the experimental group were collected with cotton swabs, washed with phosphate buffer saline (PBS), centrifuged at 5000 × g for 5 min, and the supernatant was discarded. The bottom CA cells were diluted with PBS buffer, incubated with 50.0 μL PI (100 μg/mL) staining solution at room temperature for 30 min, resuspended in 1.0 mL PBS buffer, centrifuged at 5000 × g for 5 min, and then suspended in 1.0 mL PBS buffer. The fungal suspension was coated on the slide, and the staining of CA was observed and photographed with a fluorescence microscope (LEICA, DM4B, Germany) under green excitation light. The numbers of fluorescent CA cells and hyphae in each group were statistically analyzed. A fungal solution treated with sterile water was used as the blank control.

Histology Assay

After the final administration for 24 h, the vaginas of mice in each group were subjected to lavage with normal saline and the mice were immediately sacrificed. Each vagina was isolated, placed in 10% formalin solution for 24 h, and the container was sealed with paraffin. Sections (4.0 μm thickness) were separately stained with PAS and H&E, and then observed and photographed under an inverted microscope (Nikon, Tokyo, Japan).

Cytokine Detection

The vaginal tissues in each group on day 16 were excised, and homogenized with a glass homogenizer in normal saline at 2000 rpm for 15 min to collect the supernatant. The amounts of TNF-α, IL-6, IL-1β and IL-10 were measured by enzyme-linked immunosorbent assay kits (Dakewe, Beijing, China).[23]

Data Analysis

The obtained data were expressed as mean values ± SD, and analyzed by *t* test using Origin 9.0 pro software.

Results

Solubility of NYS

To increase the drug loading of nanoemulsions, the maximum solubility of NYS in oil phase and co-emulsifier was screened. The results (Figure 1) showed higher NYS solubility in paraffin oil and PEG400, 0.73 ± 0.08 mg/mL and 3.35 ± 0.17 mg/mL, respectively. Therefore, paraffin oil and PEG400 were selected as the oil phase and co-emulsifier.

Preparation and Optimization of Nanoemulsions

The preparation of nanoemulsions was optimized by response surface method. By investigating the influence of independent variables (NYS content, ultrasonic treatment time, and ultrasonic amplitude) on droplet size, the optimal combination of these three independent variables was confirmed. The reference solubility of NYS was set at 300, 500, and 700 μg/mL, ultrasonic times were set at 5, 10, and 15 min, and ultrasonic amplitudes were set at 15%, 25%, and 35% (amplitude limit of 40%).

Table 2 shows the horizontal design of the full factorial design (3^3) for each independent variable, as well as the mean and SD of droplet size. Droplet size ranged from 227.0 ± 8.72 nm to 312.0 ± 9.54 nm. The droplet size data were input into the software to obtain the regression model-adjusted equation. As shown in Figure 2A, the actual and predicted values were distributed near the line ($P < 0.0001$, $R^2 = 0.9794$), indicating that the model could reasonably reflect the change of response and had a good fitting degree.

The 3-D response surface diagram is shown in Figure 2B–D. As ultrasonic time and amplitude increased, the size of the liquid droplets decreased. The droplet size was minimum at a time of 15 min and amplitude of 35%. The effect of NYS content on droplet size was not significant. Based on the analysis, the optimal treatment conditions were determined as ultrasonic time of 15 min, ultrasonic amplitude of 35%, and NYS content of 700 μg/mL.

Using the optimal conditions confirmed above, the effects of EPS (0.5%, 1%, and 1.5%), PEG400 (0%, 2%,

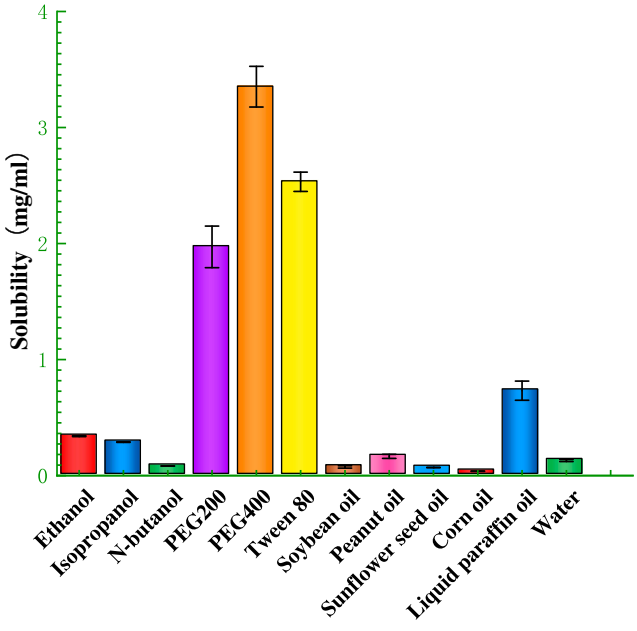

Figure 1 Solubility of NYS in various components.

Table 2 Full Factorial Design with Three Independent Variables (NYS, Time and Amplitude) and the Experimental Response (Droplet Size) for the Process Optimization

Std	Independent Variables			Response Variable
	X_1	X_2	X_3	Y_1
1	300	5	15	311 ± 3
2	700	5	15	312 ± 9.54
3	500	5	15	311 ± 33.51
4	300	10	15	291 ± 7
5	700	10	15	288 ± 7.81
6	500	10	15	285 ± 4
7	300	15	15	283 ± 8.54
8	500	15	15	275 ± 2.65
9	700	15	15	279 ± 8.19
10	700	5	25	304 ± 2
11	300	5	25	306 ± 7
12	500	5	25	305 ± 8.72
13	300	10	25	279 ± 7.81
14	700	10	25	277 ± 2.65
15	500	10	25	276 ± 7
16	700	15	25	242 ± 3.61
17	500	15	25	251 ± 10.44
18	300	15	25	245 ± 1.73
19	300	5	35	285 ± 4.58
20	700	5	35	284 ± 4.58
21	500	5	35	285 ± 4.58
22	500	10	35	254 ± 2
23	300	10	35	253 ± 2
24	700	10	35	255 ± 2.65
25	300	15	35	234 ± 1.73
26	500	15	35	235 ± 8.72
27	700	15	35	227 ± 8.72

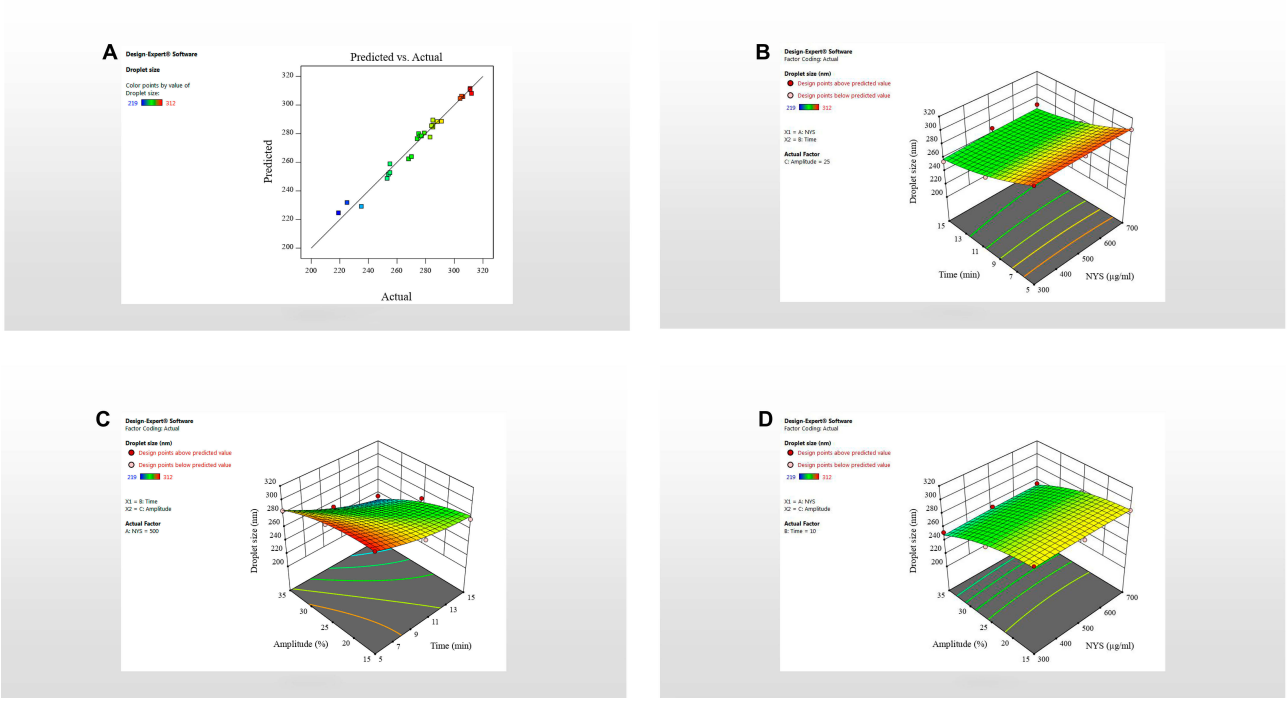

Figure 2 (**A**) Comparison of the predicted and experimental for the Y_1 values of the ENNE. R^2 = coefficient of determination. Response surface plot showing the interaction effect for droplet size as a function of (**B**) NYS concentration (X_1), (**C**) ultrasonic time (X_2), and (**D**) ultrasonic amplitude (X_3).

and 4%) and liquid paraffin oil (5%, 10% and 15%) on the nanoemulsions were next investigated. A new full factorial design (3^3 + 5) was carried out on 32 samples, as shown in Table 3. Nonlinear regression analysis was performed on particle size, zeta potential, inhibition zone, and release degree, and the results were used to establish a mathematical model (Table 4 Y1/Y2/Y3/Y4) to draw a 3-D response diagram, as shown in Figure 3A–I.

The response surface results (Figure 3A–C) indicated that as the content of EPS and PEG400 increased, the particle size of the droplets decreased. Droplet size increased with liquid paraffin oil content. The content of PEG400, EPS, and liquid paraffin oil all increased with inhibition zone (Figure 3D–F). The in vitro release of NYS increased with PEG400 content (Figure 3G–I), but decreased with increased content of EPS and liquid paraffin oil.

The optimization scheme and actual values for nanoemulsions prepared by the ultrasonic method are shown in Table 5.

Characterization of ENNE

According to the optimized formulation and condition, the obtained ENNE had a translucent off-white appearance (Figure 4A). Emulsion type identification showed faster and more uniform spread of the water-soluble methylene blue in the nanoemulsion system (Figure 4B). The Sudan III gathered into drops, with diffusion that was slow and uneven (Figure 4C). Based on these results, ENNE was classified as an O/W type emulsion.

Average particle size, zeta potential, and viscosity of ENNE were measured at pH=4.5 (to simulate the vaginal environment). The data presented in Figure 4D and E illustrated that the average particle size of ENNE was 131.1 ± 4.32 nm, the polydispersity index (PDI) was 0.083, the zeta potential was −36.9 MV, and the dynamic viscosity was 115.8 ± 4.5 mPa·s, the EE was 97.3%. TEM (Figure 4H and I) illustrated that the microscopic morphology of the ENNE droplets was more like an encapsulated structure, with uniform distribution and no aggregation.

DSC and TG

The DSC and TG results are shown in Figure 5A and showed an endothermic peak for NYS at 130.1°C (ΔH 4.46 mJ). This peak is the melting peak of NYS, and indicates that NYS is crystallized before it becomes a nanoemulsion. NYS showed a second endothermic peak at 172.7°C, and the TG value decreased, indicating that NYS decomposed in the temperature range of 163.7–185.8°C. There was no significant difference in the endothermic peak value of NYS between 126.1°C and

Table 3 Full Factorial Design with Three Independent Variables (X_4: EPS, X_5: PEG400 and X_6: Liquid Paraffin Oil) and the Experimental Responses (Y_1: Droplet Size; Y_2: Zeta Potential; Y_3: Inhibition Zone and Y_4: NYS Released in 1h) for Process Optimization

Std	Independent Variables			Response Variables			
	X_4	X_5	X_6	Y_1	Y_2	Y_3	Y_4
1	0.5	0	5	209 ± 3.61	−37.4 ± 0.4	1190 ± 0	5.9 ± 0.7
2	0.5	0	5	227 ± 4	−35.4 ± 0.5	2380 ± 0	7.5 ± 1.6
3	0.5	4	5	145 ± 3.46	−37.2 ± 1.1	600 ± 0	14.1 ± 1.6
4	0.5	8	5	139 ± 6.08	−39.1 ± 0.7	600 ± 0	14.7 ± 3.1
5	0.5	0	15	234 ± 6.08	−36.7 ± 0.3	1810 ± 0	8.3 ± 1.4
6	0.5	4	15	221 ± 8.72	−38.6 ± 0.4	910 ± 0	12.1 ± 0.6
7	0.5	8	15	223 ± 11.53	−40.4 ± 0.3	910 ± 0	12.8 ± 1.5
8	0.5	0	25	264 ± 15.72	−38.1 ± 1.1	1510 ± 0	5.2 ± 0.9
9	0.5	0	25	265 ± 12.49	−38.4 ± 0.6	1510 ± 0	5.4 ± 1.1
10	0.5	4	25	234 ± 8.89	−39.9 ± 1	750 ± 0	11.3 ± 1
11	0.5	8	25	234 ± 6.08	−41.8 ± 0.8	750 ± 0	13.3 ± 0.9
12	1	0	5	196 ± 7	−34.3 ± 0.3	1190 ± 0	6.1 ± 1.6
13	1	4	5	149 ± 5.29	−36.2 ± 0.8	600 ± 0	12.6 ± 1.7
14	1	8	5	137 ± 2	−38.9 ± 1	600 ± 0	13.1 ± 0.6
15	1	8	5	138 ± 3.61	−38.1 ± 0.4	600 ± 0	13.9 ± 2
16	1	0	15	253 ± 6.56	−35.7 ± 1	1810 ± 0	5.7 ± 1.1
17	1	4	15	216 ± 5.29	−37.5 ± 0.4	910 ± 0	11.8 ± 0.7
18	1	4	15	212 ± 5.2	−37.9 ± 0.8	910 ± 0	11.4 ± 0.8
19	1	8	15	189 ± 4.58	−39.4 ± 0.4	910 ± 0	14.2 ± 1.1
20	1	0	25	252 ± 9	−37 ± 1	3020 ± 0	5.9 ± 0.5
21	1	4	25	239 ± 3.46	−38.9 ± 0.8	750 ± 0	10.1 ± 2.9
22	1	4	25	236 ± 7.21	−38.9 ± 0.5	750 ± 0	10.7 ± 1.7
23	1	8	25	226 ± 10.44	−40.7 ± 0.7	750 ± 0	13.9 ± 1.6
24	1.5	0	5	187 ± 6.24	−34.4 ± 0.2	1190 ± 0	7.1 ± 1.7
25	1.5	4	5	141 ± 2	−35.2 ± 1	600 ± 0	12.9 ± 1.8
26	1.5	8	5	130 ± 5	−36.9 ± 0.5	910 ± 0	14.1 ± 0.6
27	1.5	0	15	231 ± 13.23	−34.7 ± 0.2	1810 ± 0	5.9 ± 0.6
28	1.5	4	15	203 ± 3.61	−36.5 ± 0.7	910 ± 0	10.6 ± 0.9
29	1.5	8	15	188 ± 7.94	−40.4 ± 0.4	910 ± 0	12.4 ± 0.8
30	1.5	0	25	247 ± 7.94	−36 ± 1	3020 ± 0	6.1 ± 1.6
31	1.5	4	25	231 ± 5.29	−37.8 ± 0.3	750 ± 0	10.9 ± 1.2
32	1.5	8	25	215 ± 6.56	−39.7 ± 0.6	750 ± 0	12.8 ± 1.5

130.1°C after making the nanoemulsion preparation. The endothermic peak at 126.1°C becomes flat and the peak area decreases (ΔH of 0.12 mJ). The second endothermic peak value of ENNE group was not evident at 163.7–185.8 °C, indicating that the decomposition temperature of NYS in ENNE increased and the thermal stability was enhanced.

Storage Stability and pH Stability

No phase separation occurred after storage of ENNE for 10 weeks, and the average particle size increased from 131.0 ± 4.32 nm to 315.0 ± 5.5 nm (Figure 5B), indicating high storage stability. As shown in Figure 5C, at pH = 2, two peaks appeared in the particle size distribution for ENNE at 227.0 ± 5.12 nm and 4496.0 ± 19.32 nm. At pH = 3–7, the range of particle size changed slightly (from 207.0 ± 6.5 nm to 131.0 ± 4.32 nm).

In vitro Drug Release

The result of in vitro release (Figure 6) demonstrated that the cumulative release of ENNE reached 69.0 ± 3.2% at 24 h, and continued to increase until 60 h. The cumulative release of NYS/oil and NYS/water at 24 h was below 55.9% ± 5.0, and showed no additional increase from 24 h to 60 h. ENNE exhibited a stronger release capacity with a significant slow-release effect. After model fitting, the Higuchi equation gave the biggest r value (r = 0.949)

Table 4 Summary of Regression Analysis for Responses Variables

Responses Variables	Regression Model: $Y=a + bx_4 + cx_5 + dx_6 + ex_4x_5 + fx_4x_6 + gx_5x_6 + hx_4^2 + ix_5^2 + jx_6^2$									
	a	b	c	d	e	f	g	h	i	j
Y_1	211.03	−8.45	−22.83	38.44	0.0944	1.15	9.38	−1.79	11.75	−17.42
Y_2	−36.10858	1.95464	−0.455542	−0.118192	–	–	–	–	–	–
Y_3	14.38	0.0995	2.81	0.9376	−0.1006	0.0732	−0.4582	0.3098	−1.33	0.6559
Y_4	11.52	−0.2654	3.62	−0.6579	−0.1103	0.0922	0.0469	0.2513	−1.92	0.1264
Batch	**R^2**		**Adjusted R^2**	**Predicted R^2**		**SD**		**CV%**		**P > F**
Y_1	0.9627		0.9474	0.9222		9.39		4.54		< 0.0001
Y_2	0.9283		0.9206	0.9022		0.5463		1.45		< 0.0001
Y_3	0.9628		0.9476	0.9219		0.6000		4.27		< 0.0001
Y_4	0.9519		0.9323	0.9026		0.8488		8.16		< 0.0001

for ENNE. Thus, the release mechanism could be explained mathematically according to the following Equation (2):

$$\frac{Mt}{M\infty} = kt^{\frac{1}{2}} \quad (2)$$

Where "t" is the release time; "Mt/M∞" is the percentage of the drug released at "t"; "k" is the release constant. Here, $k = 11.44186 \pm 0.6$.

Anti-CA in vitro

MIC

The MIC of ENNE was determined using a double dilution method. The results indicated that the MICs of NYS/oil and NYS/water (free NYS) were 4.0 μg/mL and 4.0 μg/mL, respectively, and that of ENNE was only 0.125 μg/mL.

Inhibition Zone

The inhibition zone measurements (Figure 7A) indicated ENNE (19.0 ± 0.5 mm) > amphotericin B (18.4 ± 0.7 mm) > NYS/oil (11.0 ± 0.5 mm) > NYS/water (10.0 ± 0.5 mm) > blank emulsion (0). For a drug content of 35.0 μg/mL, ENNE exhibited stronger fungal inhibition, which was attributed to the larger dispersion degree and increased surface area of ENNE.

SEM

SEM was performed and revealed that CA cells in the ENNE group were significantly different from normal CA. As illustrated in Figure 7B and C, whole CA cells were fully oval shaped, and those after treatment appeared wrinkled or shrunken.

Animal Experiments

In vivo Dynamic Antifungal Activity

On the 5th day of ENNE treatment, redness and swelling were alleviated, and secretions decreased. After 10 days, the swelling and secretion disappeared. In the positive control group, the redness and swelling decreased gradually on the 5th day, but did not disappear until the 15th day, so the cure time was longer. There was no mortality recorded during the treatment period.

The numbers of CA in the vagina of mice were measured regularly. The result showed (Figure 7D) that, after nine days of treatment, the amounts of fungal cells in the vaginal lavage fluid of the experimental group and the positive control group gradually decreased to below 10^3 CFU/mL.

PI Staining

Microscopically, CA in the secretions entered the mycelium phase. According to PI staining, both CA cells and mycelia in the normal group showed no red fluorescence (Figure 7E and F), while ENNE group showed 98.9% red fluorescence (Figure 7G and H) and nifuratel-NYS vaginal cream group showed 73.4% red fluorescence (Figure 7I and J).

PAS Staining

Compared with the normal group (Figure 8A), there were dense CA cells and hyphae in the model group vagina (Figure 8B). After 10 days of administration, CA cells and mycelia in the vagina of the ENNE group all disappeared (Figure 8C). However, there were still residual CA cells in the vaginal folds of the positive control group (Figure 8D).

H&E Staining

H&E staining showed that the overall structure of the vaginal tissue in the normal group appeared normal, with

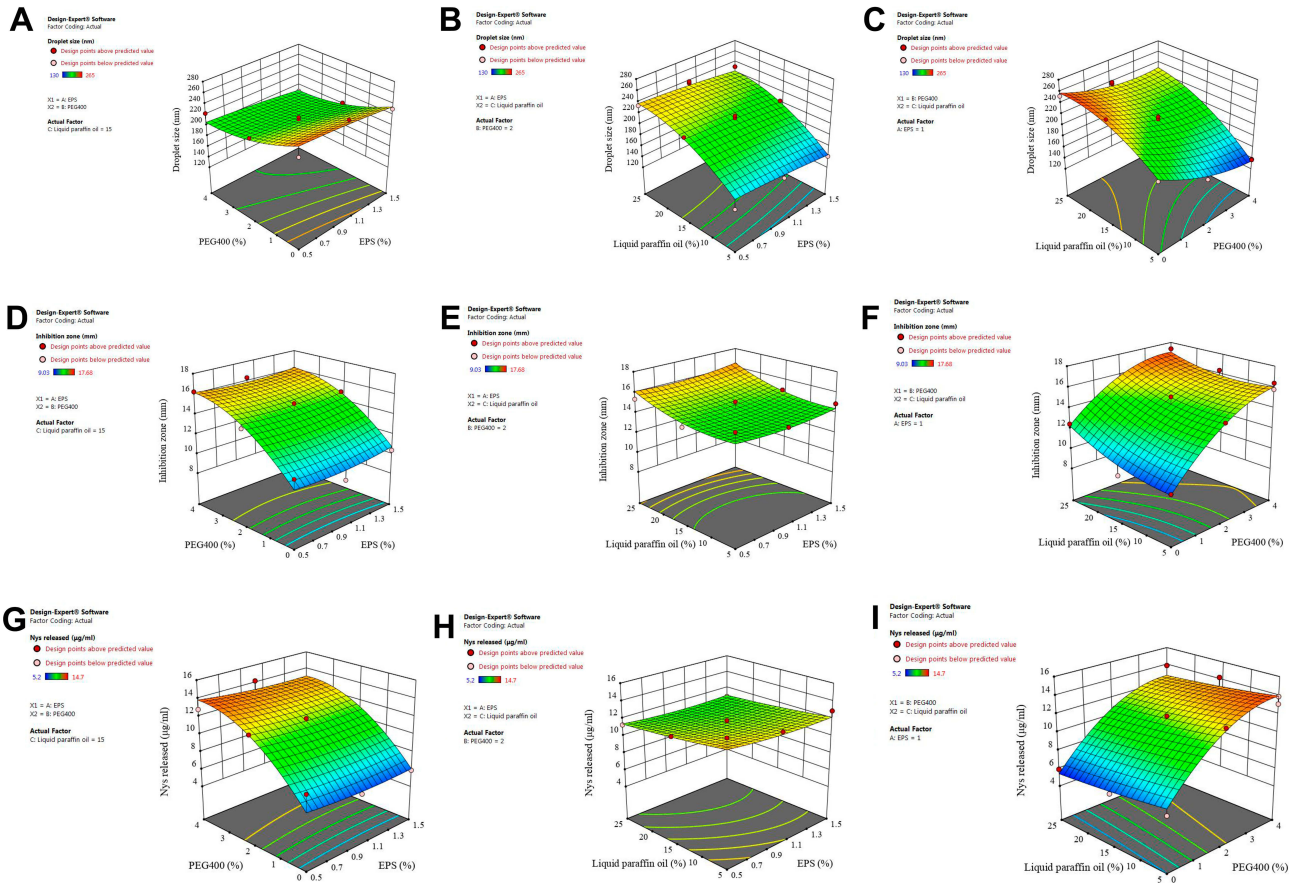

Figure 3 3-D Response surface plots showing the interaction effect for droplet size (**A-C**), inhibition zone (**D-F**), and NYS released in 1h (**G-I**) as a function of NYS in EPS (X4), PEG400 (X5), and liquid paraffin oil (X6).

no inflammatory cell infiltration and complete keratinization (Figure 9A). Obvious tissue degeneration and inflammatory cell infiltration were observed in the model group, indicating successful modeling (Figure 9B). In the treatment group, the flat upper layer of the vaginal lamina was not completely keratinized, and there was no inflammatory cell infiltration (Figure 9C). In the positive control group, the flat upper layer of the vaginal lamina was not completely keratinized, and the count of inflammatory cells was significantly reduced (Figure 9D).

ELISA Assays for Inflammatory Factors

ELISA was next used to detect secretion levels of inflammatory factors TNF-α, IL-1β, IL-6, and IL-10 in the vaginal tissues of VVC mice in each group. As shown in Figure 10A–D, the levels of all the inflammatory factors were elevated in the model group. After ENNE treatment, there was significantly lower secretion of TNF-α, IL-1β, IL-6, and IL-10 than that of the positive control group (* $P<0.05$). The results indicated that ENNE could effectively reduce the secretion of inflammatory factors to improve VVC inflammation.

Discussion

The use of EPS has great application potential in emulsifiers, but its use has not been reported in nanoemulsions. In this study, an EPS/NYS nanoemulsion was prepared by

Table 5 Optimization Scheme and Actual Values

Batch	Independent Variables						Dependent Variables			
	X_1	X_2	X_3	X_4	X_5	X_6	Y_1	Y_2	Y_3	Y_4
Predicted	700	15	35	1.5	3.22134	5.0	128.545	−36.7	15.875	13.4419
Experimental	700	15	35	1.5	3.2	5	131 ±4.32	−36.9 ± 0.3	18.4 ± 0.7	12.2 ± 0.12

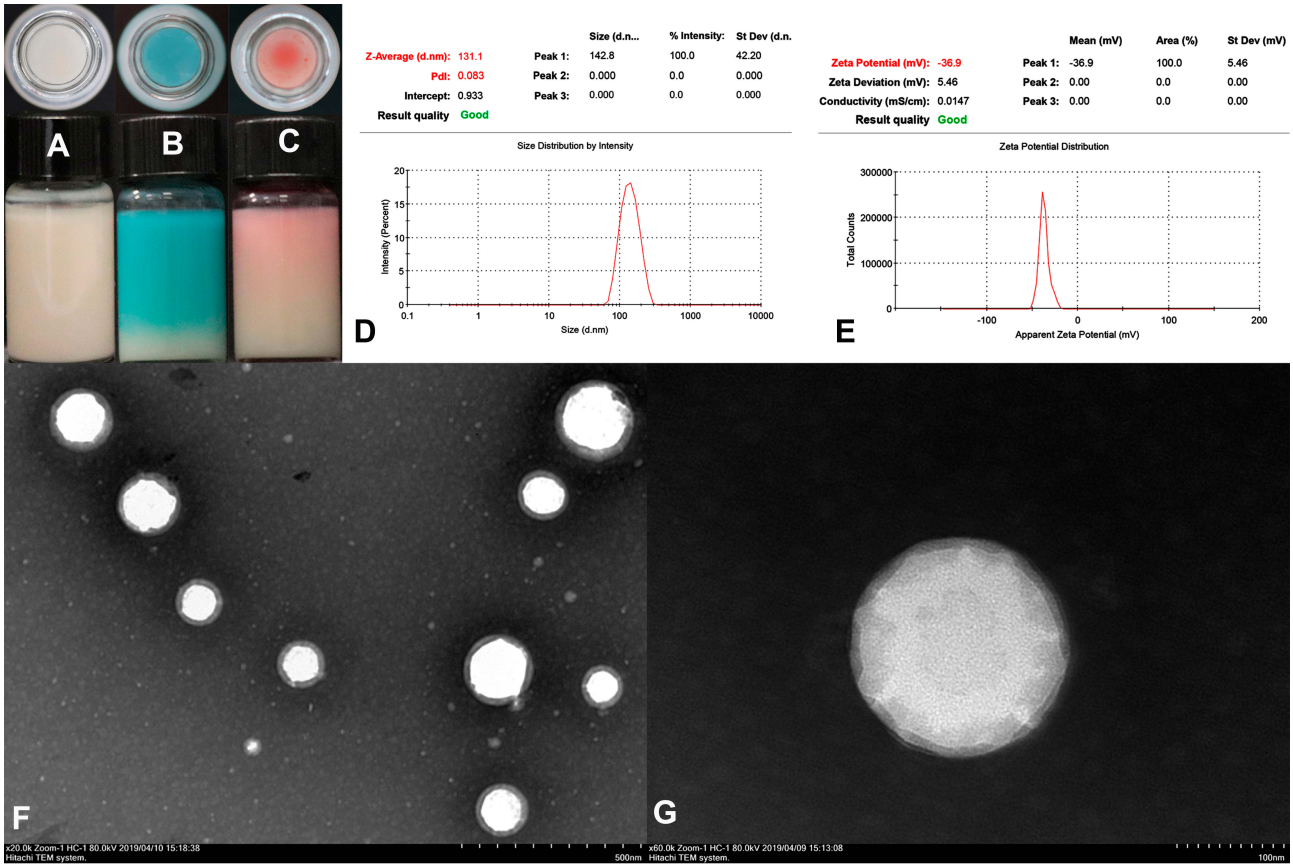

Figure 4 (**A**) ENNE; (**B**) Methylene blue stain photos; (**C**) Sudan III stain photos; (**D**) Droplet size and distribution of ENNE; (**E**) Zeta potential and distribution; (**F**) TEM images × 500 nm; (**G**) TEM images × 100 nm.

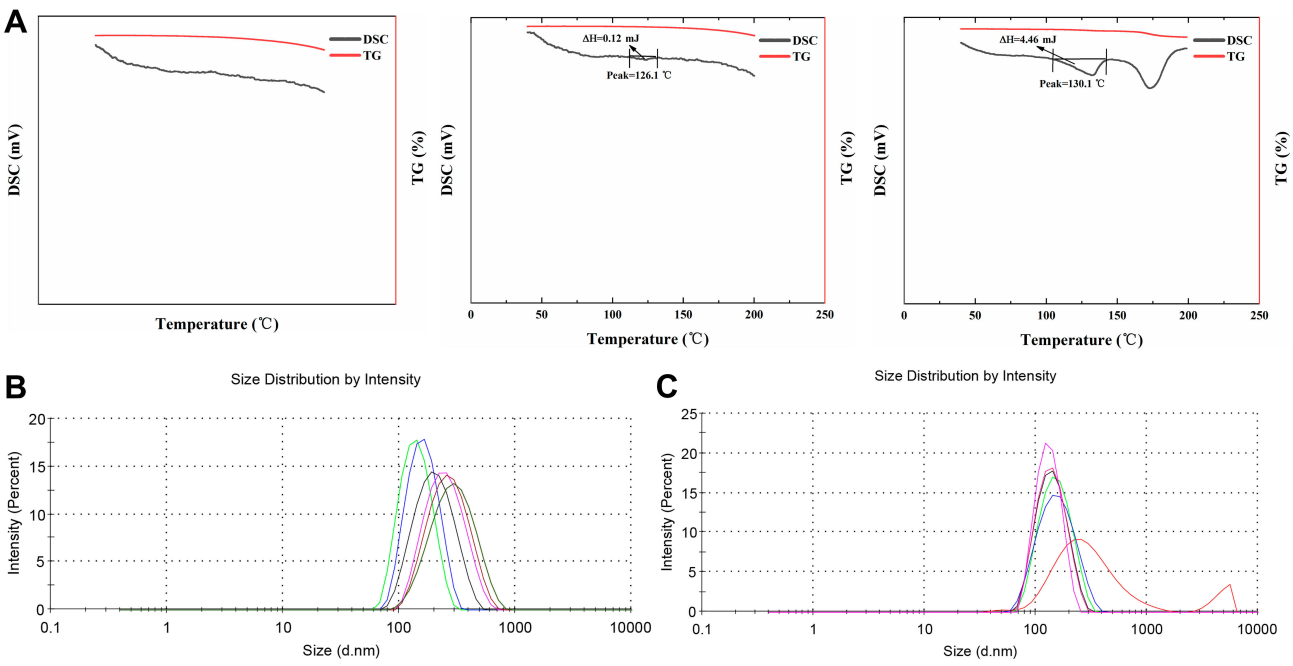

Figure 5 (**A**) DSC and TG of NYS, blank nanoemulsion and ENNE; (**B**) Storage stability of ENNE; (**C**) Stability under different pH conditions.

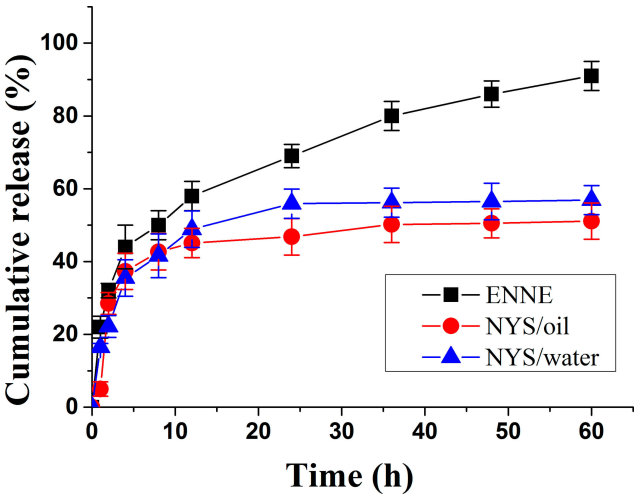

Figure 6 In vitro release profiles of ENNE compared to free NYS.

ultrasonic method using EPS as emulsifier for the first time, and optimized by response surface method to enhance the anti-CA effect and therapeutic ability against VVC of NYS.

Prior to formulation development, the oil, surfactant, and co-surfactant must be selected.[15] All long chain fatty acids (vegetable oils) showed poor NYS solubilizing potential. Medium chain fatty acids (liquid paraffin oil) solubilized the maximum amount of NYS. PEG400 (Polyethylene glycol-400) exhibited the highest solubilizing capacity, followed by Tween-80 and other surfactants. These results are similar to those reported by Ahmed et al.[13] Therefore, liquid paraffin oil and PEG400 were selected as the oil phase and co-emulsifier, respectively, improving the solubilization, release, and stability of the prepared nanoemulsions.

ENNE was prepared by ultrasonic method. High power ultrasonic cavitation can disrupt intermolecular forces in solution, destroy interfacial tension, disperse water or oil at the lower end of the probe, and reduce droplet size.[25] The preparation of ENNE was then optimized by response surface method. Since many factors are involved in the formulation and ultrasonic treatment of the nanoemulsion, full factorial design

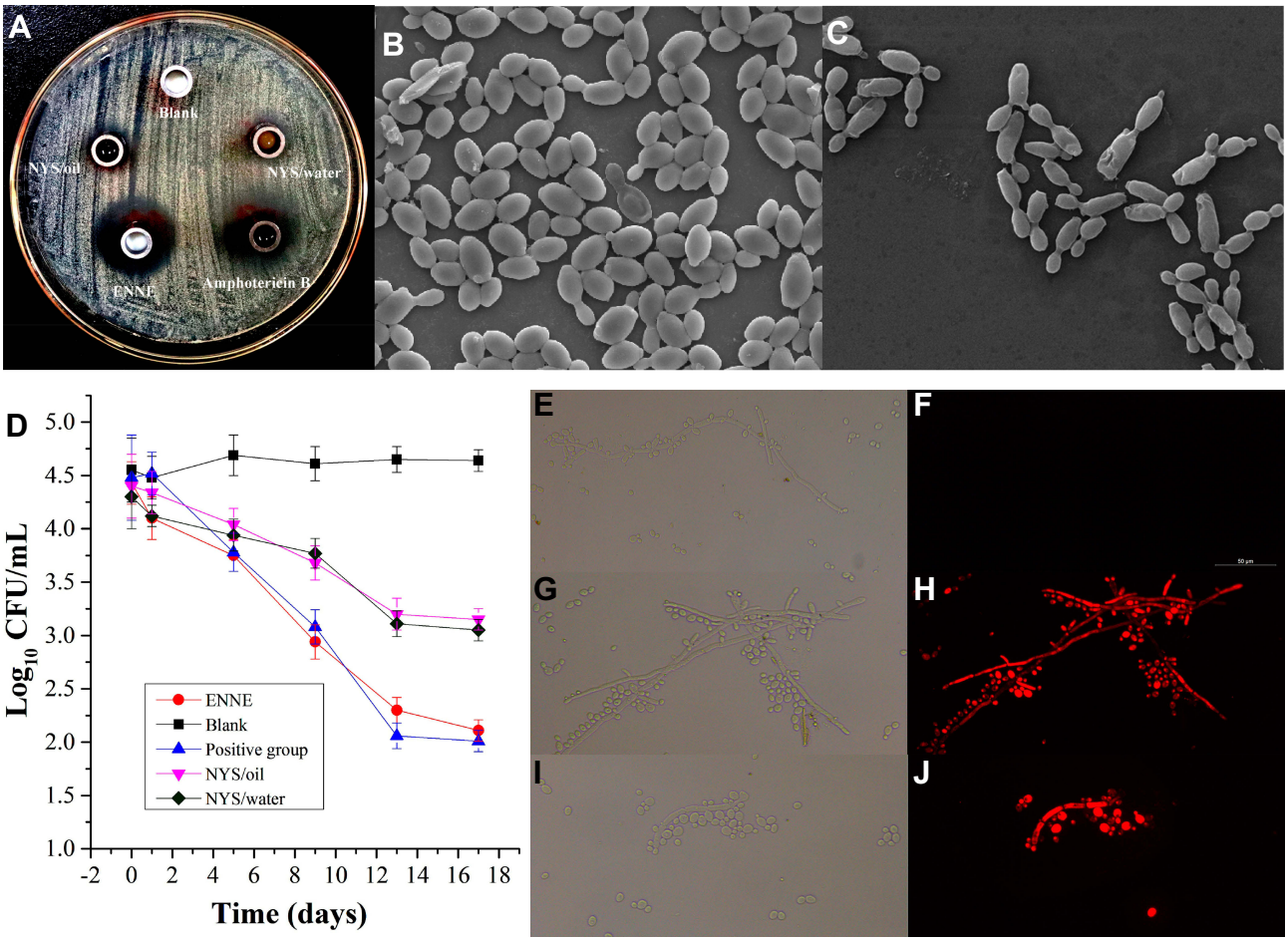

Figure 7 (**A**) Inhibition zone; (**B**) SEM images of normal CA cells; (**C**) SEM images of CA cells after ENNE action; (**D**) Dynamic antifungal curve in the vagina of mice (data presented as mean ± S.D, n=6); (**E**) white-light photographs of CA strains stained by PI in the blank control group; (**F**) fluorescence photos of CA strains stained with PI in blank control group; (**G**) white image of CA strain stained by PI after ENNE treatment; (**H**) fluorescence images of CA strain stained by PI after ENNE treatment; (**I**) white image of CA strain stained by PI after nifuratel-NYS vaginal cream treatment; (**J**) fluorescence images of CA strain stained by PI after nifuratel-NYS vaginal cream treatment.

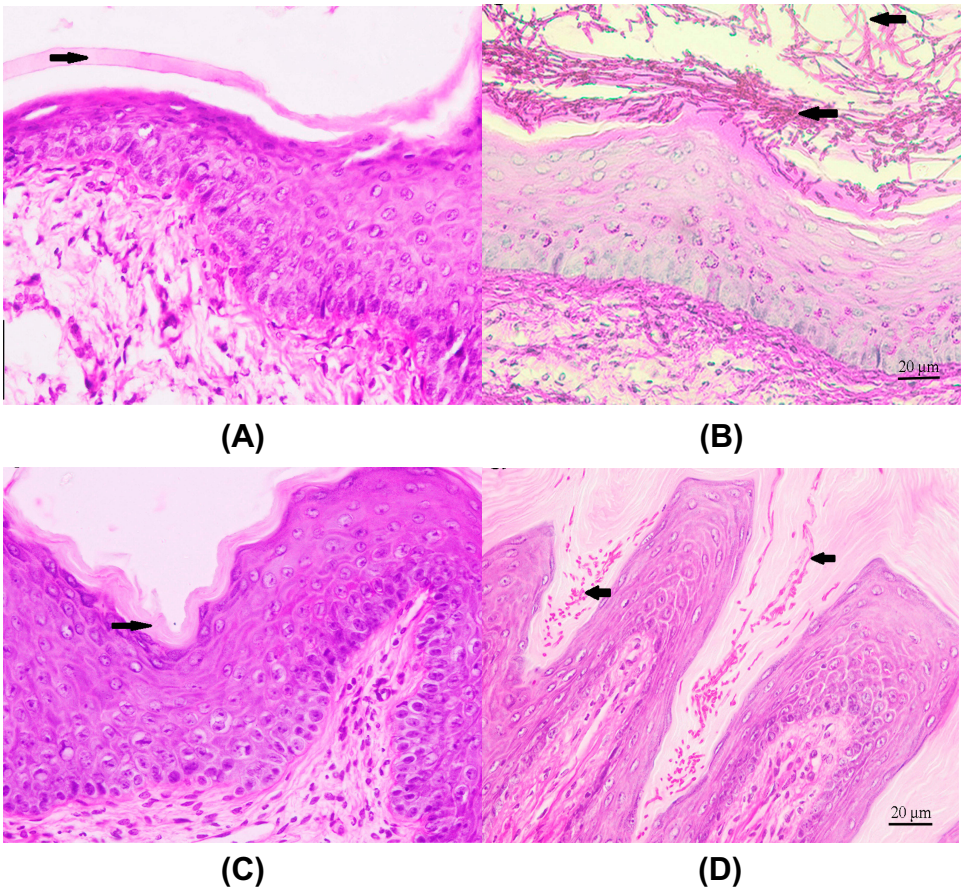

Figure 8 Images of PAS staining: (**A**) Normal group; (**B**) Model group; (**C**) ENNE group; (**D**) Positive control group. ("→" indicate complete keratinization; "←" indicate CA cells and mycelia in the vagina).

allows determination of the interactions between various factors. Although other designs (Box-Behnken Design: BBD and Central Composite Design: CCD) require less energy and time, these cannot fully reflect the interaction of multiple independent variables.[12] The response surface results showed that the particle size of liquid droplets increased with the proportion of oil phase. This may be because the viscosity of the oil phase affected the ultrasonic efficiency and restricted the reduction in particle size.[26] Drug release from emulsions is mainly determined by the transfer rate between oil and water phases, i.e. the rate at which the drug diffuses from the oil phase through the water-oil membrane into the water phase.[27] The increase in EPS and liquid paraffin oil resulted in decreased NYS release. This was attributed to the significantly increased droplet size and the decreased surface area caused by increased oil content, which limited drug release. The increase in PEG400 led to an increase in NYS release. This phenomenon was attributed to the change of oil–water interface curvature caused by the increased PEG400 content, which reduced particle size, increased surface area, and promoted drug release. At the same time, NYS has good solubility in PEG400, and the increased PEG400 content helps the drug cross the oil-water membrane to promote the drug release.[15]

The ultrasonic preparation of nanoemulsions is simple and rapid, and the response surface method is an effective and reasonable method to optimize and screen the best preparation conditions and formulations. Previous studies have employed similar approaches to optimization. For example, Ahmed et al used a response surface method to optimize agomelatine nanoemulsions prepared by ultrasound, with an average particle size of only 73.72 ± 2.53 nm.[13] Mohammadi et al applied mucilage extracted from leaves of *Pereskia aculeata* Miller as an emulsifier, and the average particle size was only 116.0 nm based on ultrasound-assisted preparation and responsive surface optimization.[28] Shanmugapriya et al prepared astaxanthin-α tocopherol nanoemulsions with an average particle size of 106.0–213.7 nm using the same method.[29]

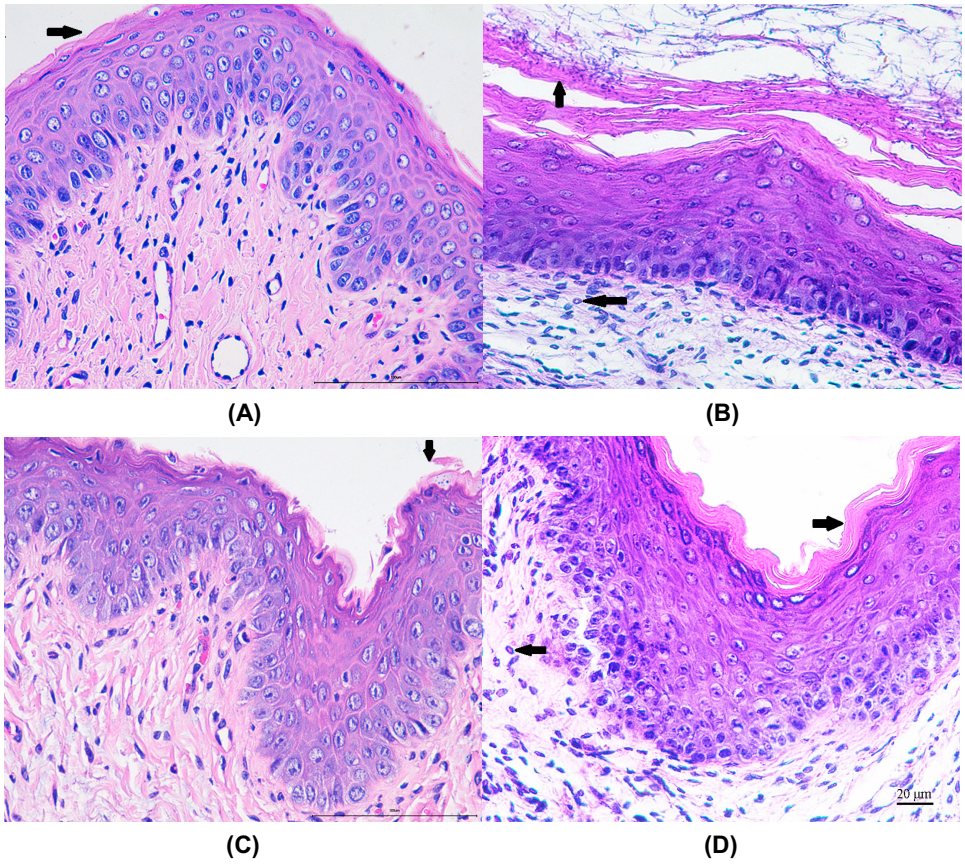

Figure 9 Images of H&E staining: (**A**) Normal group; (**B**) Model group; (**C**) ENNE group; (**D**) Positive control group. ("→" indicate complete keratinization; "←" indicates inflammatory cell infiltration; "↑" indicates tissue degeneration; "↓" indicates the flat upper layer of the vaginal lamina was not completely keratinized).

The prepared ENNE was an O/W type emulsion. The water-soluble nature of EPS makes it more likely to form an O/W emulsion. The properties of the emulsifier influence the type of emulsion. Generally, water-soluble emulsifiers contribute to the formation of O/W emulsions.[30] The average particle size, PDI and zeta potential data of ENNE indicating that the particle size distribution was relatively narrow and uniform. The zeta potential shows that the ENNE is in a stable range. The moderate dynamic viscosity is favorable to ductility and fluidity.[31] The encapsulated structure of ENNE might provide some protective and slow-release effects on the encapsulated active compound. This is the first report on the structure of EPS nanoemulsions.

DSC and TG results indicated that NYS does not react, and NYS was completely dissolved in ENNE, no NYS precipitated, and the thermal stability of NYS was improved. This is due to the solubilization effect of the nanoemulsion, which causes NYS to change from a crystalline state to an ionic state.[15] Brownian motion of the nanoemulsion droplets overcomes the influence of gravity, thus preventing separation and aggregation to greatly increase the stability.[32] Additionally, a large number of hydroxyl groups on the surface of EPS and PEG400 molecules cause steric hindrance between particles, which effectively restrict the free movement of particles to prevent particle coalescence.[33] Generally, the pH of the normal vaginal environment ranges between 3.8 and 4.5. ENNE can maintain stability within this range with little influence on particle size, allowing drug release at a constant rate.

In vitro drug release results showed that ENNE showed a certain slow-release effect. Generally, the smaller the size of the nanoemulsion and the larger the specific surface area, the faster the release rate of the drug and the larger the cumulative release.[28] The large specific surface area of ENNE promotes the release of NYS. Additionally, the solidified membrane encapsulated by oil droplets acts as a physical barrier shell, which slows drug release. This slow-release effect can prolong the duration of drug action as well as improve overall efficacy and bioavailability. For example, NYS-loaded PLGA-Glucosamine nanoparticles prepared by Mohammadi et al exhibited a slow-release effect, reaching accumulative release of 80% at 10 h.[28]

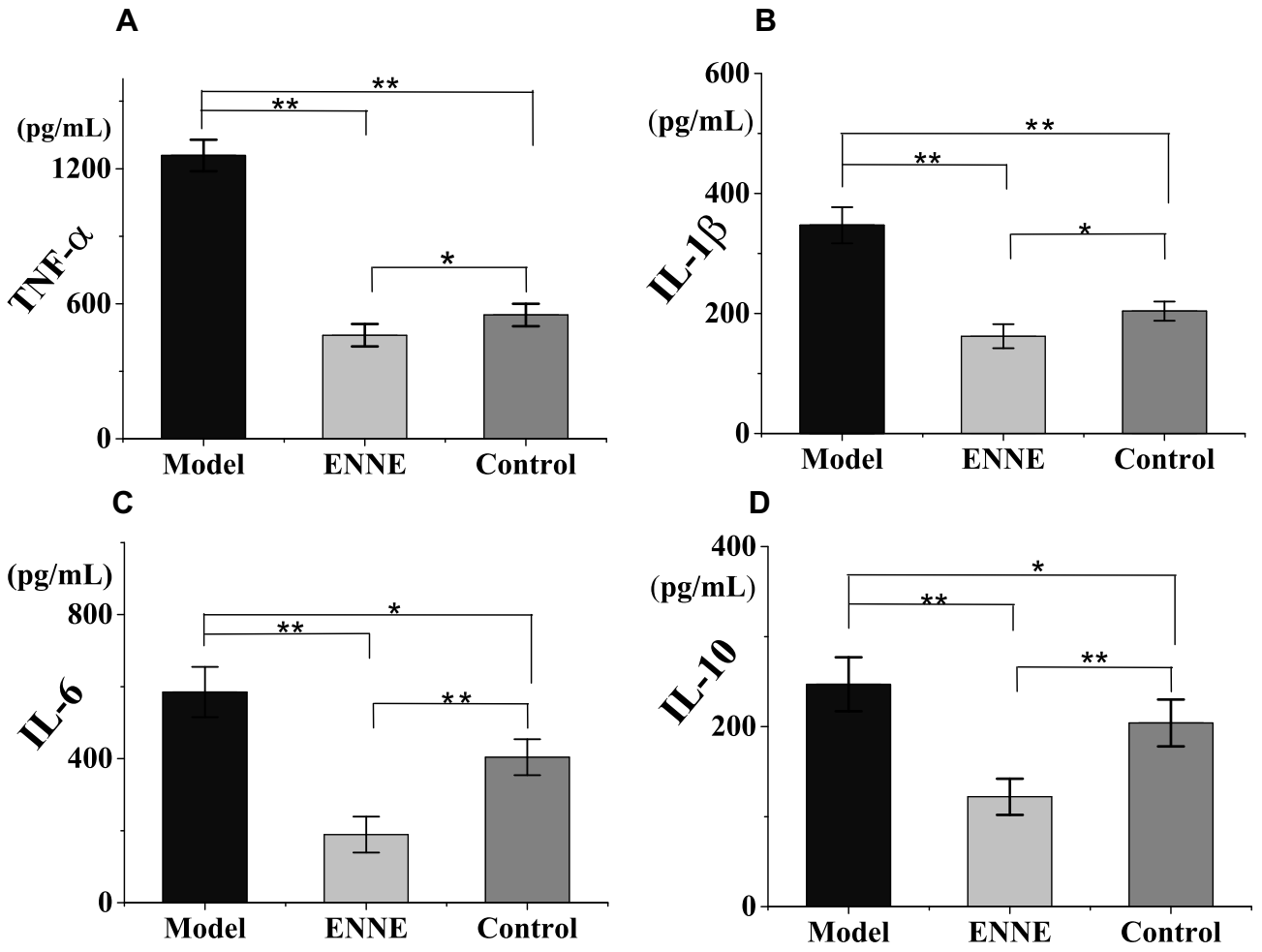

Figure 10 Effects of ENNE on the secretion of inflammatory factors in the vaginal tissues of VVC mice: (**A**) TNF-α, (**B**) IL-1β, (**C**) IL-6, and (**D**) IL-10 (*P < 0.05, **P < 0.01).

The MIC of ENNE was only 1/32 of the free NYS. The dispersibility and surface area of ENNE droplets were greatly increased. Good dispersion and fluidity increase the mobility of drug molecules, and even dispersion increases the chance that the drug can contact the CA, resulting in enhanced antifungal effect.[34] Similarly, Kassem et al used oleic acid, Tween 20, and dimethyl sulfoxide to prepare a self-nanoemulsifying drug delivery system (SNEDDS). After encapsulating NYS, the MIC was 0.256 μg/mL, indicating that the solubilization and nanosizing enhanced drug absorption.[21] The reported MIC of NYS transdermal nanoemulsion prepared by Fernández-Campos et al was 0.78 μg/mL, and could effectively treat candidiasis.[5] ENNE group exhibited a bigger inhibition zone. The small inhibition zone in the NYS/water group is due to the poor water solubility and aggregation tendency of NYS. The relatively small inhibition zone in the NYS/oil group reflects the difficulty of NYS molecules to cross the oil–water interface. In conclusion, according to MIC and inhibition zone experiments, ENNE significantly enhanced the anti-CA ability of NYS. In addition, the ENNE-treated CA cell wall appeared wrinkled or shrunken. This phenomenon is consistent with the antifungal mechanism of NYS. NYS can inhibit the synthesis of ergosterol, an important component of the fungal cell membrane, resulting in decreased integrity of the membrane to inhibit fungal survival and reproduction.[35]

During the animal experiment, the vaginal orifice of mice in the model group showed obvious redness and swelling, with more white and thick secretions, indicating successful modeling. Transformation of yeast into the mycelium phase is a necessary process for CA to induce disease, and is required for the success of modeling. Mycelia promote adhesion of CA to the mucosal surface and formation of biofilm, thus enhancing the pathogenic capacity of CA and intensifying local inflammation.[36,37] In vivo anti-CA results showed that although the drug content in ENNE was only 1/70 the amount administered to the positive control group, the antifungal effect was basically the same. PI staining results are

consistent with membrane damage to CA cells or increased permeability after ENNE action, further demonstrating the mechanism of NYS to alter the cell membrane. PI dyes are unable to enter living cells, and instead enter fungi through the membranes of dead cells, where they embed DNA to release fluorescence.[22] PAS staining and H&E staining results indicated that ENNE could better adapt to the special environment and structure of the vagina to avoid fungal residue in the folds of the vaginal mucosa. PAS dye reacts specifically with cellulose in the fungal wall to stain the fungus red or a purplish-red color.[38]

In summary, in vivo and in vitro anti-CA, VVC, animal, and cytokine experiments indicate an improved therapeutic effect of ENNE. The dispersion and surface area of ENNE droplets is larger, resulting in a larger drug action area. The moderate viscosity of ENNE makes it easier to spread in the vagina and enter the folds to kill residual fungi. EPS not only acts as an emulsifier in the emulsion, but also enhances the adhesion of tissues due to its natural biological adhesion, which increases the retention of drug in the vaginal epithelium and extends the action time.[39–41] Hydrophilic groups in the EPS can interact with mucin molecules present in the mucus, leading to bioadhesive bonds.[39] EPS is a natural nontoxic and non-irritating polysaccharide with good biocompatibility, which will facilitate meeting the requirements for product safety, patient compliance, and long-term treatment.[42] In addition, NYS can enhance the immune response to CA and protect the ultrastructure of the vaginal epithelium.[43] Above all, ENNE has certain advantages and strong application potential for the treatment of local fungal infections due to its nanoscale particle size, excellent mobility, pH stability, slow release, and biological adhesion.

Conclusion

To address the disadvantages of NYS, O/W-type nanoemulsions ENNE were prepared by ultrasound treatment due to the excellent emulsifying activity of EPS. The obtained ENNE with encapsulated structure had smaller particle size, higher storage stability, pH stability, as well as sustained-release capability. In vitro analysis of the anti-CA activity showed that the prepared ENNE exhibited improved resistance to CA. Finally, animal experiments, PI, PAS, H&E staining, and cytokine experiments all indicated that ENNE exhibited good antifungal and therapeutic ability against VVC in vivo. This study provides the foundation for future development and application of NYS nanoemulsion preparation for the treatment of VVC and provides general guidance for applications of EPS in nanoemulsions.

Acknowledgments

This work was supported by National Science Foundation of China (No. 81903568 and No. 81870237). We are thankful to the Key Laboratory of Pharmacology of Weifang Medical University.

Disclosure

The authors report no conflicts of interest in this work.

References

1. Bradford LL, Ravel J. The vaginal mycobiome: a contemporary perspective on fungi in women's health and diseases. *Virulence*. 2017;8(3):342–351. doi:10.1080/21505594.2016.1237332
2. Pappas PG, Kauffman CA, Andes DR, et al. Executive summary: clinical practice guideline for the management of candidiasis: 2016 update by the infectious diseases society of America. *Clin Infect Dis*. 2015;62(4):409–417. doi:10.1093/cid/civ1194
3. Consolaro M, Martins H, Da Silva M, et al. Efficacy of fluconazole and nystatin in the treatment of vaginal candida species. *Acta Derm Venereol*. 2012;92(1):78–82. doi:10.2340/00015555-1194
4. Kaur IP, Kakkar S. Topical delivery of antifungal agents. *Expert Opin Drug Deliv*. 2010;7(11):1303–1327.
5. Fernández-Campos F, Clares Naveros B, López Serrano O, et al. Evaluation of novel nystatin nanoemulsion for skin candidosis infections. *Mycoses*. 2013;56(1):70–81. doi:10.1111/j.1439-0507.2012.02202.x
6. Johal HS, Garg T, Rath G, Goyal AK. Advanced topical drug delivery system for the management of vaginal candidiasis. *Drug Deliv*. 2016;23(2):550–563. doi:10.3109/10717544.2014.928760
7. Soriano-ruiz JL, Calpena-capmany AC, Cañadas-enrich C, et al. Biopharmaceutical profile of a clotrimazole nanoemulsion: evaluation on skin and mucosae as anticandidal agent. *Int J Pharm*. 2019;554:105–115. doi:10.1016/j.ijpharm.2018.11.002
8. Rai VK, Mishra N, Yadav KS, Prasad N. Nanoemulsion as pharmaceutical carrier for dermal and transdermal drug delivery: formulation development, stability issues, basic considerations and applications. *J Control Release*. 2018;270:203–225. doi:10.1016/j.jconrel.2017.11.049
9. Kumar S, Ali J, Baboota S. Design Expert® supported optimization and predictive analysis of selegiline nanoemulsion via the olfactory region with enhanced behavioural performance in Parkinson's disease. *Nanotechnology*. 2016;27:43. doi:10.1088/0957-4484/27/43/435101
10. Satpute SK, Banat IM, Dhakephalkar PK, et al. Biosurfactants, bioemulsifiers and exopolysaccharides from marine microorganisms. *Biotechnol Adv*. 2010;28(4):436–450. doi:10.1016/j.biotechadv.2010.02.006
11. Li C, Zhou L, Yang H, et al. Self-assembled exopolysaccharide nanoparticles for bioremediation and green synthesis of noble metal nanoparticles. *ACS Appl Mater Interfaces*. 2017;9:22808–22818. doi:10.1021/acsami.7b02908
12. Lago AMT, Neves ICO, Oliveira LN, Botrel DA, Minim LA, De Resende JV. Ultrasound-assisted oil-in-water nanoemulsion produced from *Pereskia aculeata* Miller mucilage. *Ultrason Sonochem*. 2018;50:339–353. doi:10.1016/j.ultsonch.2018.09.036
13. Ahmed S, Gull A, Alam M, et al. Ultrasonically tailored, chemically engineered and "QbD" enabled fabrication of agomelatine nanoemulsion; optimization, characterization, ex-vivo, permeation and stability study. *Ultrason Sonochem*. 2017;41:213–226. doi:10.1016/j.ultsonch.2017.09.042
14. Song B, Zhu WJ, Song RT, Yan F, Wang Y. Exopolysaccharide from *Bacillus vallismortis* WF4 as an emulsifier for antifungal and antipruritic peppermint oil emulsion. *Int J Biol Macromol*. 2019;125:436–444. doi:10.1016/j.ijbiomac.2018.12.080

15. Sosa L, Clares B, Alvarado HL, Bozal N, Domenech O, Calpena AC. Amphotericin B releasing topical nanoemulsion for the treatment of candidiasis and aspergillosis. *Nanomedicine*. 2017;13(7):2303–2312. doi:10.1016/j.nano.2017.06.021
16. Desai P, Patlolla RR, Singh M. Interaction of nanoparticles and cell-penetrating peptides with skin for transdermal drug delivery. *Mol Membr Biol*. 2010;27(7):247–259. doi:10.3109/09687688.2010.522203
17. Mahtab A, Anwar M, Mallick N, Naz Z, Jain GK, Ahmad FJ. Transungual delivery of ketoconazole nanoemulgel for the effective management of onychomycosis. *AAPS PharmSciTech*. 2016;17(6):1477–1490. doi:10.1208/s12249-016-0488-0
18. Shanmugam A, Ashokkumar M. Ultrasonic preparation of stable flax seed oil emulsions in dairy systems physicochemical characterization. *Food Hydrocoll*. 2014;39:151–162. doi:10.1016/j.foodhyd.2014.01.006
19. Malik T, Chauhan G, Rath G, Kesarkar RN, Chowdhary AS, Goyal AK. Efavirenz and nano-gold-loaded mannosylated niosomes: a host cell-targeted topical HIV-1 prophylaxis via thermogel system. *Artif Cell Nanomed Biotechnol*. 2017;46(sup1):79–90. doi:10.1080/21691401.2017.1414054
20. Shao Y, Wu C, Wu T, et al. Eugenol-chitosan nanoemulsions by ultrasound-mediated emulsification: formulation, characterization and antimicrobial activity. *Carbohydr Polym*. 2018;193:144–152. doi:10.1016/j.carbpol.2018.03.101
21. Kassem AA, Mohsen AM, Ahmed RS, Essam TM. Self-nanoemulsifying drug delivery system (SNEDDS) with enhanced solubilization of Nys for treatment of oral candidiasis: design, optimization, in vitro and in vivo evaluation. *J Mol Liq*. 2016;218:219–232. doi:10.1016/j.molliq.2016.02.081
22. Song B, Rong YJ, Zhao MX, Chi ZM. Antifungal activity of the lipopeptides produced by *bacillus amyloliquefaciens* anti-ca against *candida albicans* isolated from clinic. *Appl Microbiol Biotechnol*. 2013;97(16):7141–7150. doi:10.1007/s00253-013-5000-0
23. Jin L, Bai X, Luan N, et al. A designed tryptophan and lysine/arginine-rich antimicrobial peptide with therapeutic potential for clinical antibiotic-resistant *Candida albicans* vaginitis. *J Med Chem*. 2016;59(5):1791–1799. doi:10.1021/acs.jmedchem.5b01264
24. Mirza MA, Ahmad S, Mallick MN, Manzoor N, Talegaonkar S, Iqbal Z. Development of a novel synergistic thermosensitive gel for vaginal candidiasis: an in vitro, in vivo evaluation. *Colloids Surf B Biointerfaces*. 2013;103:275–282. doi:10.1016/j.colsurfb.2012.10.038
25. Gao H, Hu G, Liu K, Wu L. Preparation of waterborne dispersions of epoxy resin by ultrasonic-assisted supercritical CO_2, nanoemulsification technique. *Ultrason Sonochem*. 2017;39:520–527. doi:10.1016/j.ultsonch.2017.05.032
26. Piorkowski DT, Mcclements DJ. Beverage emulsions: recent developments in formulation, production, and applications. *Food Hydrocoll*. 2014;42:5–41. doi:10.1016/j.foodhyd.2013.07.009
27. Washington C. Drug release from microdisperse systems: a critical review. *Int J Pharm*. 1990;58(1):1–12. doi:10.1016/0378-5173(90)90280-H
28. Mohammadi G, Shakeri A, Fattahi A, et al. Preparation, physicochemical characterization and anti-fungal evaluation of nystatin-loaded PLGA-glucosamine nanoparticles. *Pharm Res*. 2016;34(2):1–9. doi:10.1007/s11095-016-2039-5
29. Shanmugapriya K, Hyejin K, Sivagnanam SP, et al. Astaxanthin-alpha tocopherol nanoemulsion formulation by emulsification methods: investigation on anticancer, wound healing, and antibacterial effects. *Colloid Surf B Biointerfaces*. 2018;172:170–179. doi:10.1016/j.colsurfb.2018.08.042
30. Wang Y, Ahmed Z, Feng W, et al. Physicochemical properties of exopolysaccharide produced by *lactobacillus kefiranofaciens* zw3 isolated from tibet kefir. *Int J Biol Macromol*. 2008;43(3):283–288. doi:10.1016/j.ijbiomac.2008.06.011
31. Brugués AP, Naveros BC, Calpena CAC, et al. Developing cutaneous applications of paromomycin entrapped, in stimuli-sensitive block copolymer nanogel dispersions. *Nanomedicine*. 2015;10(2):227–240. doi:10.2217/nnm.14.102
32. Schmitt M. Active brownian motion of emulsion droplets: coarsening dynamics at the interface and rotational diffusion. *Eur Phys J E Softer Matter*. 2016;39(8):80. doi:10.1140/epje/i2016-16080-y
33. Li X, Qin Y, Liu C, et al. Size-controlled starch nanoparticles prepared by self-assembly with different green surfactant: the effect of electrostatic repulsion or steric hindrance. *Food Chem*. 2016;199:356–363. doi:10.1016/j.foodchem.2015.12.037
34. Mcclements DJ, Rao J. Food-Grade nanoemulsions: formulation, fabrication, properties, performance, biological fate, and potential toxicity. *Crit Rev Food Sci Nutr*. 2011;51(4):285–330. doi:10.1080/10408398.2011.559558
35. Coutinho A, Prieto M. Cooperative partition model of nystatin interaction with phospholipid vesicles. *Biophys J*. 2003;84(5):3061–3078. doi:10.1016/S0006-3495(03)70032-0
36. Gulati M, Nobile CJ. *Candida albicans* biofilms: development, regulation, and molecular mechanisms. *Microbes Infect*. 2016;18(5):310–321. doi:10.1016/j.micinf.2016.01.002
37. Carmen RC, Miguel CG, Alberto MV, et al. Biofilms and vulvovaginal candidiasis. *Colloid Surf B Biointerfaces*. 2019;174:110–125. doi:10.1016/j.colsurfb.2018.11.011
38. Luca AD, Carvalho A, Cunha C, et al. Il-22 and ido1 affect immunity and tolerance to murine and human vaginal candidiasis. *PLoS Pathog*. 2013;9(7):e1003486. doi:10.1371/journal.ppat.1003486
39. Bassi P, Kaur G. Bioadhesive vaginal drug delivery of nystatin using a derivatized polymer: development and characterization. *Eur J Pharm Biopharm*. 2015;96:173–184. doi:10.1016/j.ejpb.2015.07.018
40. Martín-villena MJ, Fernández-campos F, Calpena-campmany AC, et al. Novel microparticulate systems for the vaginal delivery of nystatin: development and characterization. *Carbohydr Polym*. 2013;94(1):1–11. doi:10.1016/j.carbpol.2013.01.005
41. Onkar S, Tarun G, Goutam R, et al. Microbicides for the treatment of sexually transmitted HIV infections. *J Pharm*. 2014;2014:1–18.
42. Song B, Song R, Cheng M, Chu H, Yan F, Wang Y. Preparation of calcipotriol emulsion using bacterial exopolysaccharides as emulsifier for percutaneous treatment of psoriasis vulgaris. *International Journal of Molecular Sciences*. 2019;21(1):77. doi:10.3390/ijms21010077
43. Zhang X, Li T, Chen X, Wang S, Liu Z. Nystatin enhances the immune response against *candida albicans* and protects the ultrastructure of the vaginal epithelium in a rat model of vulvovaginal candidiasis. *BMC Microbiol*. 2018;18:166. doi:10.1186/s12866-018-1316-3